

CURRENT-INDUCED SUPERCONDUCTOR-INSULATOR TRANSITION IN GRANULAR HIGH- T_c SUPERCONDUCTORS

Y. Kopelevich*, C. A. M. dos Santos**, S. Moehlecke*, and A. J. S. Machado**

(*) *Instituto de Física "Gleb Wataghin", Universidade Estadual de Campinas, Unicamp 13083-970, Campinas, São Paulo, Brasil*

(**) *Departamento de Engenharia de Materiais, FAENQUIL, 12600-000, Lorena, São Paulo, Brasil*

I. INTRODUCTION

The occurrence of either superconducting or insulating state in a zero-temperature limit ($T \rightarrow 0$) under variation of system parameters such as, for instance, microscopic disorder in homogeneous thin films [1–5] or charging energy/Josephson energy ratio in granular superconductors [6,7], is one of the fundamental problems in the condensed matter physics which continuously attracts an intense research interest. It has also been shown both theoretically [8] and experimentally that the superconductor-insulator transition in two-dimensional (2D) superconductors can be tuned by applied magnetic field. The field-tuned superconductor-insulator transition has been measured in amorphous [5,9–11] and granular [12] thin films, fabricated 2D Josephson-junction arrays [13,14], and bulk layered quasi-2D superconductors such as high- T_c cuprates [15,16].

On the other hand, in granular superconductors both applied magnetic field and electrical current affect the Josephson coupling between grains [17–19]. Besides, a zero-temperature current-driven dynamic transition from a vortex glass to a homogeneous flow of the vortex matter is expected to occur in disordered Josephson junction arrays [20], suggesting the intriguing possibility of a current-induced superconductor-insulator transition, analogous to the field-tuned transition [21].

In this paper we report a systematic study of electrical current effects on the superconducting properties of granular high- T_c superconductors. The here presented results demonstrate the occurrence of superconductor-insulator quantum phase transition driven by the applied electrical current, and provide evidence that the dynamics of Josephson intergranular vortices plays a crucial role in this phenomenon.

II. SAMPLES AND EXPERIMENTAL DETAILS

Polycrystalline single phase $Y_{1-x}Pr_xBa_2Cu_3O_{7-\delta}$ samples were prepared using a solid state reaction method with a route similar as described in [22] and characterized by means of x-ray powder diffractometry, and

optical and scanning electron microscopy. The analysis showed that the samples are granular materials consisting of grains with an average size $d \sim 5 \mu\text{m}$. The superconducting transition was measured both resistively and with a SQUID magnetometer MPMS5 (Quantum Design). Electrical transport dc measurements in applied magnetic field $H \leq 100$ Oe, produced by a copper solenoid, were performed using standard four-probe technique with low-resistance ($< 1 \Omega$) sputtered gold contacts. No heating effects due to current were observed for $I \leq 100$ mA, our largest measuring current. In order to eliminate thermoelectric effects, the measurements were performed inverting the applied current.

Below we present the results of measurements performed on $Y_{1-x}Pr_xBa_2Cu_3O_{7-\delta}$ sample with $x = 0.45$ close to the critical Pr concentration $x_c \approx 0.57$ above which superconductivity has not been detected [22]. The sample superconducting transition temperature (onset) $T_{c0} = 33$ K, the resistivity at the superconducting transition $\rho_N(T_{c0}) = 20$ m Ω cm, and dimensions $l \times w \times t = 12.6 \times 1.94 \times 1.24$ mm³.

III. RESULTS AND DISCUSSION

Figures 1 – 4 present the resistance vs. temperature data obtained in a vicinity of $T_{c0} = 33$ K for various applied currents and magnetic fields. As Figs. 1 – 4 illustrate, the superconducting transition temperature onset T_{c0} is both current- and field-independent. On the other hand, the zero-resistance superconducting state is destroyed by the application of both the electrical current and magnetic field.

The superconducting order parameter $\Psi = \Psi_0 e^{i\phi}$ has two components; a magnitude Ψ_0 and a phase ϕ . Because T_{c0} (and hence Ψ_0) remains unchanged, the low-temperature finite resistance in our sample originates from thermal and/or quantum fluctuations in the phase locking. In the context of granular superconductors, T_{c0} can be identified with the transition temperature of individual grains, and the phase fluctuations – with fluctuating Josephson currents between grains. In the absence of external field, the critical current is that corresponding to a vortex creation and its motion, neglecting pinning. However, in granular superconductors with a very weak coupling between grains, the Earth's magnetic field $H_E \sim 0.5$ Oe (which has not been shielded in the experiments) can easily penetrate the sample. Then, the critical

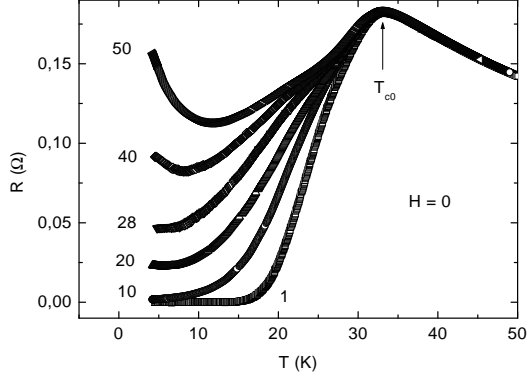


FIG. 1. Resistance $R(T) = V(T)/I$ obtained at various measuring currents (here and in Figs. 2 - 4, numbers at the curves correspond to the applied current in mA) and at no applied magnetic field.

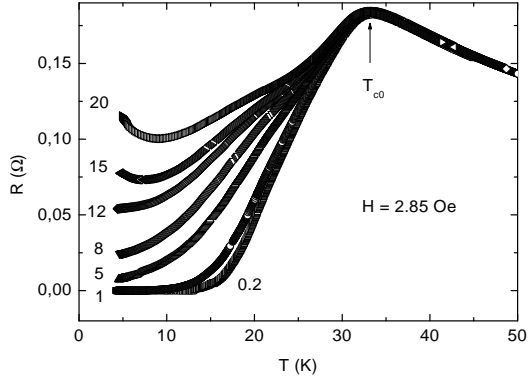


FIG. 2. Resistance $R(T) = V(T)/I$ obtained at various measuring currents and applied magnetic field $H = 2.85$ Oe.

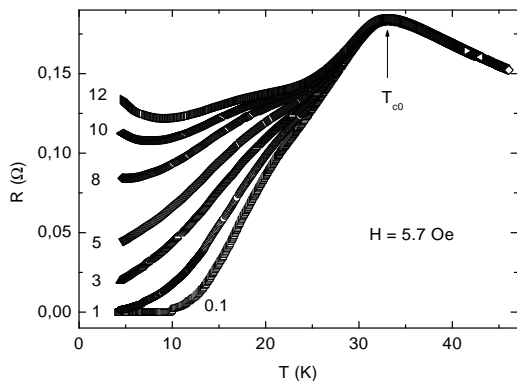


FIG. 3. Resistance $R(T) = V(T)/I$ obtained at various measuring currents and applied magnetic field $H = 5.7$ Oe.

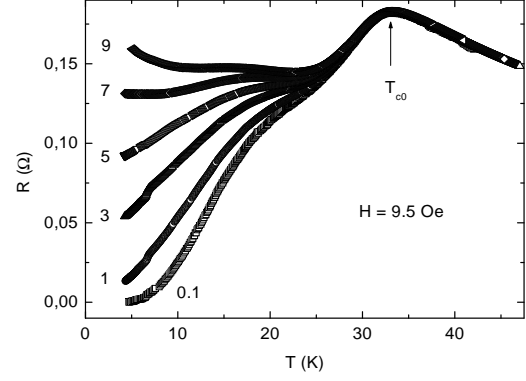


FIG. 4. Resistance $R(T) = V(T)/I$ obtained at various measuring currents and applied magnetic field $H = 9.5$ Oe.

current will be determined by the pinning of Josephson intergranular vortices originating, for example, from an inhomogeneity of the Josephson junction coupling strength.

Shown in Fig. 5 are low-current portions of current-voltage I-V characteristics measured at low temperatures and at no applied field. As can be seen from Fig. 5, the $V(I)$ dependencies can be very well described by the equation

$$V = c(T, H)(I - I_{th}(T, H))^n(T, H), \quad (1)$$

where $I_{th}(T, H)$ is the threshold current. Thus, at $T = 4.6$ K, $I_{th} = 5$ mA and the corresponding current density ($I_{th}/\text{cross section of the sample}$) $j_{th} = 0.21$ A/cm².

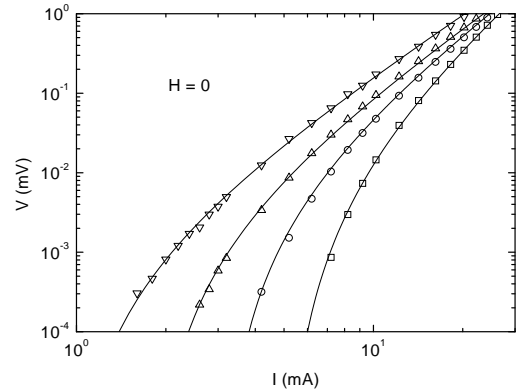


FIG. 5. Low-current portions of I-V isotherms measured at $T = 4.6$ K (\square), $T = 8$ K (\circ), $T = 11$ K (\triangle), and $T = 13$ K (∇). Solid lines are obtained from Eq. (1) with the fitting parameters $c = 0.0001$ mV/mAⁿ, $I_{th} = 5$ mA, $n = 3$ ($T = 4.6$ K); $c = 0.00025$ mV/mAⁿ, $I_{th} = 3.1$ mA, $n = 2.7$ ($T = 8$ K); $c = 0.00039$ mV/mAⁿ, $I_{th} = 1.8$ mA, $n = 2.55$ ($T = 8$ K); $c = 0.0007$ mV/mAⁿ, $I_{th} = 0.94$ mA, $n = 2.45$ ($T = 13$ K).

Within the framework of effective Josephson medium theory [23–25] one can estimate the lower critical field

$H_{c1J} \sim 8\pi^2 j_{c0} \lambda_L / c \sim 0.2$ mOe, taking the maximum Josephson current density $j_{c0} \sim 10j_{th}$ [23,26] and the typical value of the intragranular London penetration depth $\lambda_L \sim 0.1 \mu\text{m}$ ($\ll d$). The obtained value of H_{c1J} is much smaller than the Earth's magnetic field, indeed, i. e. our sample is deeply in the mixed state.

Below the threshold current $I_{th}(H,T)$ the vortex motion is strongly suppressed or zero. The I-V characteristics described by the Eq. (1) are expected in the regime where the interaction between vortices and the pinning potential dominates the vortex-vortex interaction [20,27–29].

As the applied current increases, the $V(I)$ curves approach a linear regime of flux flow where the differential resistance $R_d = dV/dI$ is current-independent, see Fig. 6. Inset in Fig. 6 exemplifies $V(I)$ measured at $T = 13$ K and demonstrates that at large enough currents the $V(I)$ can be fitted by the equation

$$V(I) = R_{ff}(I - I_{cf}). \quad (2)$$

Here R_{ff} is the flux-flow resistance and I_{cf} is the so-called dynamical critical current. In this high-current regime vortices move coherently, only weakly interacting with the pinning potential.

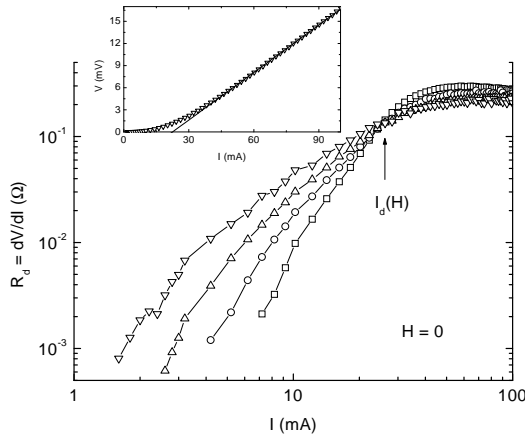


FIG. 6. Differential resistance $R_d = dV/dI$ obtained at no applied field and $T = 4.6$ K (\square), $T = 8$ K (\circ), $T = 11$ K (\triangle), and $T = 13$ K (∇). Inset shows $V(I)$ measured at $T = 13$ K; the solid line is obtained from the Eq. (1) with $R_{ff} = 0.215 \Omega$ and $I_{cf} = 22.5$ mA.

As can also be seen in Fig. 6, there exists a crossing of $R_d(I)$ curves occurring at $I = I_d$. The measurements performed at various applied fields revealed that $I_d(H)$ is a decreasing function of field. Such a crossing has also been measured in $\text{Mo}_{77}\text{Ge}_{23}$ films [30] and reproduced in numerical simulations [31] which show that the pinned fraction of vortices rapidly decreases for $I > I_d(H)$.

Figure 7 presents typical resistance hysteresis loops $R(H)$ measured at $T = 4.2$ K for various currents. These measurements were performed after cooling the sample from $T > T_{c0}$ to the target temperature in a zero applied field. As shown in Fig. 7, the resistance R cor-

responding to the increasing $|H|$ branch is larger than that corresponding to the decreasing $|H|$ branch resulting in “clockwise” $R(H)$ hysteresis loops. Previous studies [32–34] showed that the “clockwise” $R(H)$ hysteresis loops are essentially related to the granular sample structure where the resistance is determined by the motion of Josephson intergranular vortices. In increasing magnetic field larger than the first critical field of the grains ($H > H_{c1g}$), the pinning prevents Abrikosov vortices from entering the grains, and flux lines (Josephson vortices) are concentrated between grains leading to the intergrain field higher than the external applied field. When the applied field is decreased, the pinning prevents Abrikosov vortices being expelled from the grains resulting in a lower density of Josephson intergrain vortices as compared to that in the increasing field. Thus, the data of Fig. 7 provide an unambiguous evidence that the resistance in our sample is governed by the motion of intergranular Josephson vortices in both low- and high-current limits.

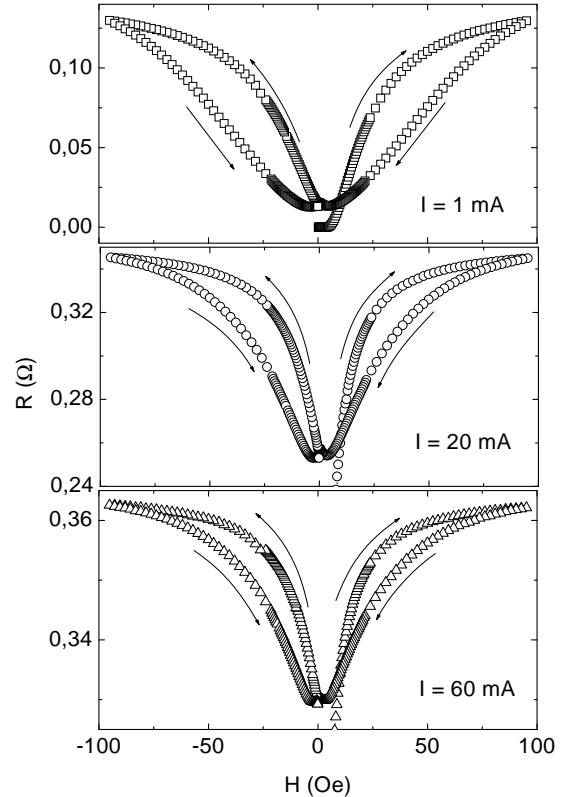


FIG. 7. $R(H)$ magnetoresistance hysteresis loops measured at $T = 4.2$ K and applied currents $I = 1$ mA, $I = 20$ mA, and $I = 60$ mA, demonstrating that the sample resistance is governed by the motion of intergranular Josephson vortices; arrows indicate the magnetic field direction in the measurements.

We note further that the resistance $R(T) = V(T)/I$ in the low-temperature limit reveals a crossover from the metallic-like ($dR/dT > 0$) to the insulating-like ($dR/dT < 0$) behavior as the applied current is increased, see Figs. 1 - 4. The results presented in Figs. 1 - 4 indicate also the existence of a field-dependent current $I_c(H)$, separating the metallic-like ($I < I_c(H)$) and insulating-like ($I > I_c(H)$) resistance curves, at which the resistance is temperature-independent. The occurrence of the temperature-independent resistance $R_c = (V/I)|_{I_c}$ can clearly be seen in Fig. 8 where a crossing of current-voltage I-V isotherms at $I_c(H)$ measured for two applied fields is shown. The inset in Fig. 8 depicts $I_c(H)$ and $I_d(H)$ which illustrates that for a given field $I_c(H) > I_d(H)$. In other words, the crossing of I-V curves takes place in the regime where the interaction between Josephson vortices dominates that with the pinning potential.

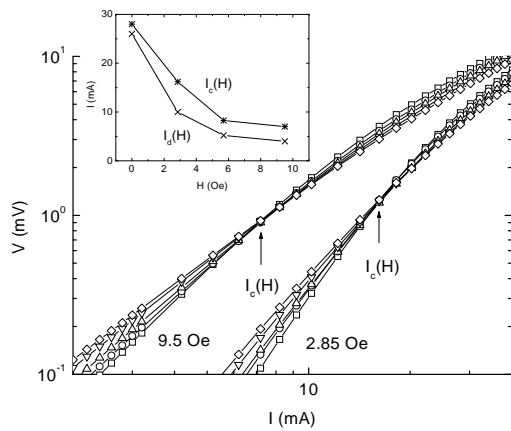


FIG. 8. Current-voltage I-V characteristics measured in applied fields $H = 2.85$ Oe and $H = 9.5$ Oe at temperatures 4.6 K (\square), 5.6 K (\circ), 6.7 K (\triangle), 8 K (∇), and 9 K (\diamond). Inset shows $I_d(H)$ and $I_c(H)$ magnetic field dependencies.

These results resemble very much the resistance behavior in a vicinity of the magnetic-field-tuned superconductor-insulator transition [9–16]. According to the theory [8], at low enough magnetic fields vortices are localized by the quenched disorder, leading to the zero-resistance ($R = 0$) superconducting state. With increasing vortex density and above some critical field H_c vortices delocalize and Bose condense, leading to the insulating state.

The theory predicts a finite-temperature scaling law [2,3,8] which allows for experimental testing of the zero-temperature superconductor-insulator transition. It is assumed in this analysis that a sample is superconductor or insulator at $T = 0$ when $dR/dT > 0$ or $dR/dT < 0$, respectively. Besides, because the magnitude of the superconducting order parameter Ψ_0 (T_{c0}) remains unchanged on each grain as the intergranular resistance $R(T, H, I)$ undergoes the transition from metallic-like to insulating-like behavior, the hard-core boson model [2,3,8] should be a good approximation in our analysis

of the superconductor-insulator transition driven by the applied current. The resistance in the critical regime of the quantum transition is given by the equation

$$R(\delta, T) = R_c f(|\delta|/T^{1/z\nu}), \quad (3)$$

where R_c is the resistance at the transition, $f(|\delta|/T^{1/z\nu})$ is the scaling function such that $f(0) = 1$, z and ν are critical exponents, and δ is the deviation of a variable parameter from its critical value. Assuming $\delta = I - I_c$ ($\delta = H - H_c$ in the case of a field-tuned transition) we plotted in Figs. 9 - 11, $R = V/I$ vs. $|\delta|/T^{1/\alpha}$ for three applied fields. In each case, the exponent α was obtained from log-log plots of $(dR/dI)|_{I_c}$ vs. T^{-1} . The expected collapse of the resistance data onto two branches distinguishing the $I < I_c$ from the $I > I_c$ data is very clear in Figs. 9 - 11.

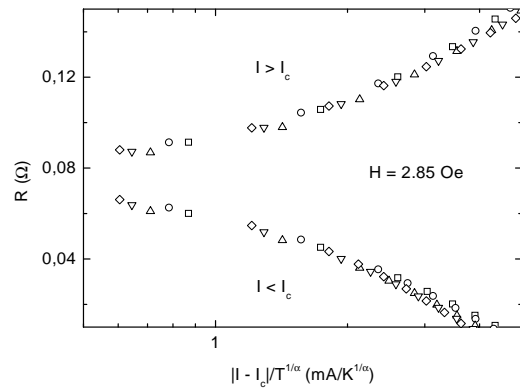


FIG. 9. Resistance $R = V/I$ as a function of the scaling variable obtained for applied field $H = 2.85$ Oe ($I_c = 16.2$ mA, $\alpha = 1.84$); $T = 4.6$ K (\square), $T = 5.6$ K (\circ), $T = 6.7$ K (\triangle), $T = 8$ K (∇).

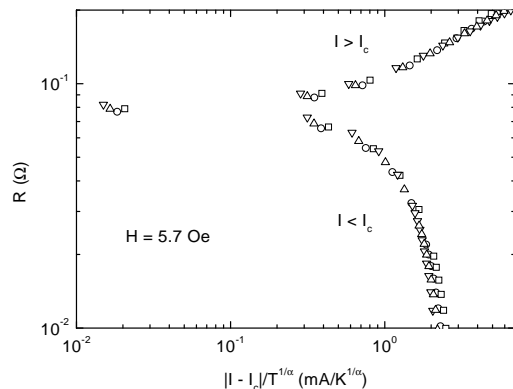


FIG. 10. Resistance $R = V/I$ as a function of the scaling variable obtained for applied field $H = 5.7$ Oe ($I_c = 8.25$ mA, $\alpha = 1.72$); $T = 4.6$ K (\square), $T = 5.6$ K (\circ), $T = 6.7$ K (\triangle), $T = 8$ K (∇).

Although, in the absence of a proper theory, the re-

sults presented in Figs. 9 - 11 should be considered as empirical ones, the very good scaling fit strongly suggests the occurrence of a zero-temperature current-induced superconductor-insulator transition. Notably, the here found exponents α agree nicely with most of the data obtained in the scaling analysis of the field-tuned transition [5,9–16].

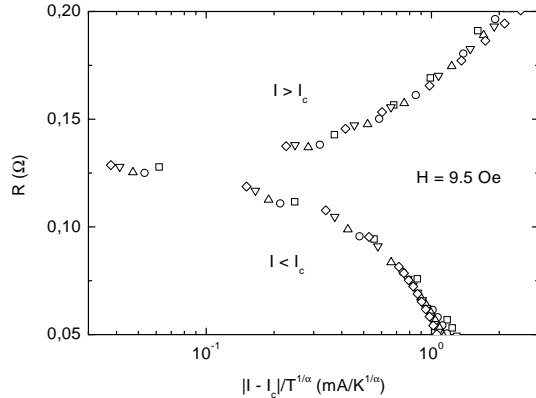


FIG. 11. Resistance $R = V/I$ as a function of the scaling variable obtained for applied field $H = 9.5$ Oe ($I_c = 7$ mA, $\alpha = 1.3$); $T = 4.7$ K (\square), $T = 5.7$ K (\circ), $T = 6.7$ K (\triangle), $T = 8$ K (∇), $T = 9$ K (\diamond).

IV. CONCLUDING REMARKS

In conclusion, we would like to emphasize that the here studied superconductor-insulator transition driven by the electrical current is essentially related to the dynamics of Josephson intergranular vortices. Actually, as the above results demonstrate, the crossing of I-V characteristics takes place in the flux flow regime. We stress that the crossover current $I_c(H)$ is smaller than the maximum supercurrent $I_0 = (2e/\hbar)E_J$ (E_J is the Josephson coupling energy) that the Josephson junctions can support. In other words, both tunneling Cooper pairs and moving Josephson vortices are present at the $I_c(H)$ which play a dual role as discussed in the context of the field-tuned transition [8].

A self-consistent analysis would require the existence of zero-temperature “depinning” transition in the Josephson vortex matter driven by the applied current. The occurrence of such a transition in disordered Josephson junction arrays has theoretically been predicted, indeed [20].

All these indicate that the current-induced superconductor-insulator transition can be considered as the dynamical counterpart of the magnetic-field-tuned transition.

Finally, we point out that similar results were obtained on $Y_{1-x}Pr_xBa_2Cu_3O_{7-\delta}$ ($x = 0.5$) and $Bi_2Sr_2Ca_{1-x}Pr_xCu_2O_{8+\delta}$ ($x = 0.54$) granular superconductors.

V. ACKNOWLEDGEMENTS

The authors would like to thank Enzo Granato for the fruitful discussions. This study was supported by FAPESP and CNPq Brazilian science agencies.

-
- [1] D. B. Haviland, Y. Liu, and A. M. Goldman, *Phys. Rev. Lett.*, **62** (1989) 2180.
 - [2] M. P. A. Fisher, G. Grinstein, and S. M. Girvin, *Phys. Rev. Lett.* **64** (1990) 587.
 - [3] M.-C. Cha, M. P. A. Fisher, S. M. Girvin, M. Wallin, and A. P. Young, *Phys. Rev. B* **44** (1991) 6883.
 - [4] Y. Liu, K. A. McGreer, B. Nease, D. B. Haviland, G. Martinez, J. W. Halley, and A. M. Goldman, *Phys. Rev. Lett.* **67** (1991) 2068.
 - [5] N. Markovic, C. Christiansen, and A. M. Goldman, *Phys. Rev. Lett.* **81** (1998) 5217.
 - [6] L. J. Geerligs, M. Peters, L. E. M. de Groot, A. Verbruggen, and J. E. Mooij, *Phys. Rev. Lett.* **63** (1989) 326.
 - [7] C. D. Chen, P. Delsing, D. B. Haviland, and T. Claeson, *Phys. Scr.* **T42**, 182 (1992).
 - [8] M. P. A. Fisher, *Phys. Rev. Lett.* **65** (1990) 923.
 - [9] A. F. Hebard and M. A. Paalanen, *Phys. Rev. Lett.* **65** (1990) 927.
 - [10] M. A. Paalanen, A. F. Hebard, and R. R. Ruel, *Phys. Rev. Lett.* **69** (1992) 1604.
 - [11] A. Yazdani and A. Kapitulnik, *Phys. Rev. Lett.* **74** (1995) 3037.
 - [12] S. Kobayashi, A. Nakamura, and F. Komori, *J. Phys. Soc. Japan* **59** (1990) 4219.
 - [13] H. S. J. van der Zant, F. C. Fritschy, W. J. Elion, L. J. Geerligs, and J. E. Mooij, *Phys. Rev. Lett.* **69** (1992) 2971.
 - [14] C. D. Chen, P. Delsing, D. B. Haviland, Y. Harada, and T. Claeson, *Phys. Rev. B* **51** (1995) 15645.
 - [15] G. T. Seidler, T. F. Rosenbaum, and B. W. Veal, *Phys. Rev. B* **45** (1992) 10162.
 - [16] S. Tanda, S. Ohzeki, and T. Nakayama, *Phys. Rev. Lett.* **69** (1992) 530.
 - [17] M. Tinkham, *AIP Conf. Proc. No. 58*, ed. by H. C. Wolfe (A. I. P. New York, 1980), p. 1.
 - [18] B. I. Belevtsev, Yu. F. Komnik, and A. V. Fomin, *J. Low Temp. Phys.* **75** (1989) 331.
 - [19] A. Gerber, T. Grenet, M. Cyrot, and J. Beille, *Phys. Rev. Lett.* **65** (1990) 3201; *Phys. Rev. B* **43** (1991) 12935.
 - [20] D. Domínguez, *Phys. Rev. Lett.* **72** (1994) 3096; *ibid.* **82** (1999) 181.
 - [21] C. A. M. dos Santos, Y. Kopelevich, S. Moehlecke, and A. J. S. Machado, *Physica C* **341-348** (2000) 1047.
 - [22] J. J. Neumeier and M. B. Maple, *Physica C* **191** (1992) 158.
 - [23] J. R. Clem, *Physica C* **153-155** (1998) 50.
 - [24] E. B. Sonin, *JETP Lett.* **47** (1988) 496.
 - [25] M. Tinkham and C. J. Lobb, “Physical Properties of the

- New Superconductors" in H. Ehrenreich and D. Turnbull (eds.) Solid State Phys. 42 (1989) 91.
- [26] C. J. Lobb, D. W. Abraham, and M. Tinkham, Phys. Rev. B 27 (1983) 150.
 - [27] P. Berghuis and P. H. Kes, Phys. Rev. B 47 (1993) 262.
 - [28] S. Bhattacharya and M. J. Higgins, Phys. Rev. Lett. 70 (1993) 2617.
 - [29] Y. Enomoto, K. Katsumi, and S. Maekawa, Physica C 215 (1993) 51.
 - [30] M. C. Hellerqvist, D. Ephron, W. R. White, M. R. Beasley, and A. Kapitulnik, Phys. Rev. Lett. 76 (1996) 4022; M. C. Hellerqvist and A. Kapitulnik, Phys. Rev. B 56 (1997) 5521.
 - [31] S. Ryu, M. Hellerqvist, S. Doniach, A. Kapitulnik, and D. Stroud, Phys. Rev. Lett. 77 (1996) 5114.
 - [32] Y. Kopelevich, V. V. Lemanov, and V. V. Makarov, Sov. Phys. Solid State 32 (1990) 2095; V. V. Makarov and Y. Kopelevich, Phys. Rev. B 54 (1996) 84.
 - [33] L. Ji, M. S. Rzchowski, N. Anand, and M. Tinkham, Phys. Rev. B 47 (1993) 470.
 - [34] S. Li, M. Fistul, J. Deak, P. Metcalf, and M. McElfresh, Phys. Rev. B 52 (1995) 747.